Proceeding Paper

Towards a Simple and Efficient Implementation of Solar Photovoltaic Emulator: An Explicit PV Model Based Approach [†]

Ambe Harrison [1],*[ID], Njimboh Henry Alombah [2][ID], Salah Kamel [3][ID], Sherif S. M. Ghoneim [4][ID], Ilyass El Myasse [5][ID] and Hossam Kotb [6][ID]

1   Department of Electrical and Electronics Engineering, College of Technology (COT), University of Buea, Buea P.O. Box 63, Cameroon
2   Department of Electrical and Electronics Engineering, College of Technology, University of Bamenda, Bambili P.O. Box 39, Cameroon; henry.alombah@gmail.com
3   Department of Electrical Engineering, Faculty of Engineering, Aswan University, Aswan 81542, Egypt; skamel@aswu.edu.eg
4   Electrical Engineering Department, College of Engineering, Taif University, P.O. Box 11099, Taif 21944, Saudi Arabia; s.ghoneim@tu.edu.sa
5   EEIS Laboratory, ENSET Mohammedia, Hassan II University of Casablanca, Casablanca 28830, Morocco; ilyaselmyasse@gmail.com
6   Department of Electrical Power and Machines, Faculty of Engineering, Alexandria University, Alexandria 21544, Egypt; hossam.kotb@alexu.edu.eg
*   Correspondence: ambe.harrison@ubuea.cm; Tel.: +237-682387064 or +237-658016181
†   Presented at the 4th International Electronic Conference on Applied Sciences, 27 October–10 November 2023; Available online: https://asec2023.sciforum.net/.

Abstract: A photovoltaic emulator (PVE) is a specialized device designed to mimic the static and dynamic properties of a solar panel. It serves as a crucial tool for testing and validating PV systems. Despite the unpredictable variations in real environmental conditions, the PVE offers a controlled environment, facilitating the smooth implementation and testing of PV subsystems. The PVE consists of two essential components: the reference PV model and the PVE power electronics controller. For simplicity, both these elements must be inherently straightforward. Numerous advanced methods have been proposed in the literature to efficiently integrate the PV model into the PVE system. However, these approaches often involve complex iterative computations of intricate equations related to solar panels, making them less practical. To address these limitations, this paper introduces a novel PVE that aims to simplify the implementation and integration of the PV model. The proposed system employs a simple and non-iterative approach to provide the reference to the PVE, using a straightforward explicit model of the solar panel. In comparison to existing works, the proposed PVE stands out for its high flexibility and simplicity as it does not require the complex iterative computations of implicit equations related to the solar panel model. The overall PVE system is implemented with a basic proportional-integral (PI) controller and a DC-DC buck power electronic converter. It is then validated using a 200 W solar panel through a series of experiments, including the EN 50530 Test. The results of these experiments demonstrate that the proposed PVE efficiently reproduces the static and dynamic characteristics of a solar panel.

Keywords: photovoltaic; photovoltaic emulator; explicit PV model; proportional-integral (PI) controller

1. Introduction

With the steady growth of the world population, ensuring accessible energy has become a pressing concern. In light of these increasing energy needs, the phasing out of fossil fuels becomes a crucial imperative for sustainability. Effectively transitioning towards renewable energy sources (RESs) emerges as an excellent strategy to combat climate change and fulfill future energy requirements [1]. Among various RSEs being sought, solar energy, through solar photovoltaics (PV), is emerging as a powerful alternative. The PV

system has received enormous attention in various recent studies [2–5]. The effective implementation of these systems requires proper validation through testing. However, controlled testing is still a challenging exercise owing to the spontaneous variations in environmental conditions [6,7]. Recently, a photovoltaic emulator (PVE) has been suggested as a potential instrument for effective and controlled testing of PV systems. A PVE is an instrument that has the potential to reproduce the characteristics of an actual solar panel. This instrument has become a key milestone in the testing and validation of PV systems. Thus, despite the uncontrolled fluctuations in actual environmental conditions, the PVE offers a controllable environment, allowing the smooth implementation and testing of PV subsystems. As a power electronics device, the controller and the reference model are two vital elements of the PVE. To enhance the simplicity of the PVE, these elements must be simple and easy to integrate within the PVE. In the literature, a number of PVEs have been proposed with unique specifications as to the integration and implementation of the reference model. The PVEs proposed in [8,9] numerically resolved the nonlinear implicit equation of the PV model in order to provide a reference to the PVE. In [10–12], a binary search algorithm is used to iteratively compute the nonlinear implicit equations of the PVE in order to provide a reference current to the PVE. The nonlinear equations of the PV model are implicit and intricate. The direct iterative computation of these equations does not only add an unwanted burden to the PVE processor, but can also considerably slow down the response of the PVE. In order to accurately emulate the actual solar panel, the PVE must be able to produce a fast dynamic response. As a consequence, the iterative computation of PV intricate equations has a huge impact on PVE accuracy and response time. In fact, the main gap identified in contemporary literature lies in the implementation and integration of the PV model within the PVE. In order to enhance the PVE, the integration of the PV model should be straightforward and simple. To address this requirement, this work introduces a novel PVE that incorporates a simple and explicit PV model integration. An explicit PV model is synthesized, allowing the easy referencing of the PVE. The overall PVE is implemented with a buck DC-DC converter and a proportional integral (PI) controller and validated on a 200 W solar panel. The rest of this paper is organized as follows: a general description of the proposed PVE is presented in Section 2. In Section 3, an explicit model of the PV is established with its integration into the PVE. The PI controller and the buck converter are presented in Section 4. The results and discussion of this paper are enumerated in Section 5, while Section 6 concludes the paper.

2. General Description of the Proposed PVE

A synoptic diagram of the proposed PVE is illustrated in Figure 1. The structure consists of a DC-DC buck converter, a PI controller, and an explicit PV model.
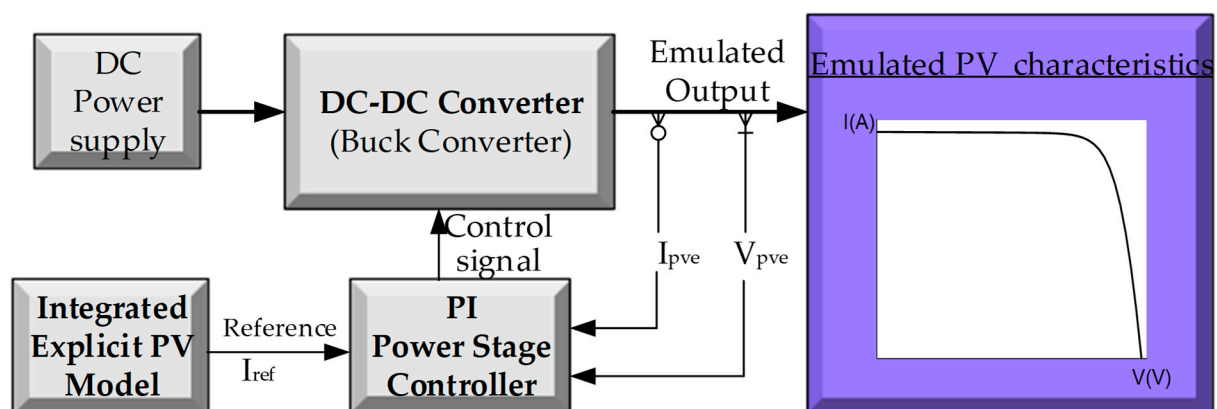

Figure 1. Synoptic diagram of the proposed PVE.

The PV model provides a reference voltage to the PI controller. The latter will regulate the DC-DC converter in order to reproduce the characteristics of the PV panel. All of these subsystems will be developed and established in the remainder of this paper.

3. Explicit PV Modeling and Integration into the PVE

The PV model is required to provide a reference to the PVE. Thus, the steady-state accuracy of the PVE heavily relies on the accuracy of the PV model. The SDM as presented in Figure 2 has been widely used in several PVE studies for its to ability to limit the complexity of the system while maintaining acceptable accuracy. It consists of a photocurrent source I_{ph}, a semiconductor diode D_1, shunt and series resistances R_{sh}, and R_s. The current-voltage $(I_{pv} - V_{pv})$ mathematical relation of this model is obtained as:

$$I_{pv} = I_{ph} - I_s \left[exp\left(\frac{(V_{pv} + I_{pv}R_s)}{a} \right) - 1 \right] - \frac{V_{pv} + I_{pv}R_s}{R_p} \tag{1}$$

where I_s is the reverse saturation current of the cell. The term $a = nN_skT/q$ such that n, N_s, T are the diode ideality factor, number of series cells, and the cell temperature respectively, while $q = 1.602 \times 10^{-19}$ C is the charge constant and $k = 1.381 \times 10^{-23}$ J/K is the Boltzmann's constant. It is evident from Equation (1) that the $(I_{pv} - V_{pv})$ relation is nonlinear and intricate. The relation is often computed implicitly to generate a reference voltage/current to the PVE [11,12]. However, such implicit computations require several iterations to converge which does not only burden the computing processor, but also slows the dynamic response of the PVE. To alleviate this challenge, this paper proposes an explicit and straightforward model of the SDM.
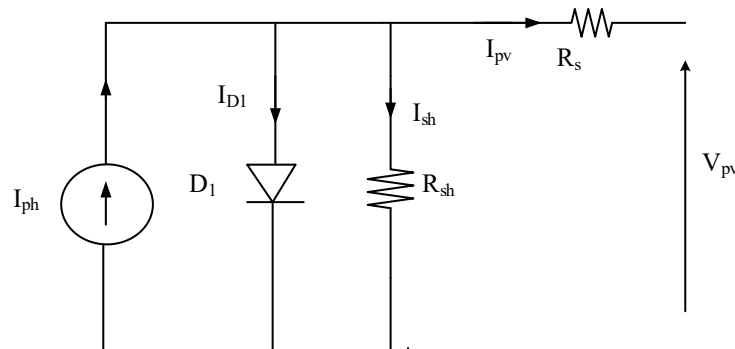

Figure 2. Electrical structure of the single diode model (SDM).

In Equation (1), a third order nonlinear approximation of the exponential term $exp\left(\frac{I_{pv}R_s}{a} \right)$ can be achieved using Taylor's series expansion as follows:

$$e^x \approx 1 + x + \frac{1}{2!}x^2 + \frac{1}{3!}x^3, x = \frac{I_{pv}R_s}{a} \tag{2}$$

Using the notion of Equation (2), Equation (1) can be converted to a cubic equation as:

$$a_1x^3 + bx^2 + cx + d = 0 \tag{3}$$

where: $a_1 = \frac{1}{6}I_sexp\left(\frac{V_{pv}}{a} \right), b = \frac{1}{2}I_sexp\left(\frac{V_{pv}}{a} \right), c = I_sexp\left(\frac{V_{pv}}{a} \right) + a\left(\frac{1}{R_s} + \frac{1}{R_{sh}} \right), d = I_sexp\left(\frac{V_{pv}}{a} \right) + \frac{V_{pv}}{R_{sh}} - I_{ph} - I_s$. In this light, Equation (3) can be solved for x, from which a straightforward determination of the PV current can be achieved using $x = \frac{I_{pv}R_s}{a}$. In line with [13], the cubic polynomial admits to a real solution if the term $B^2 - 4AC > 0$, where $A = b^2 - 3a_1c$, $B = bc - 9a_1d, C = c^2 - 3bd$. This condition is always satisfied given that $x = \frac{I_{pv}R_s}{a}$ is a unique and real value. Under this consideration, the solution to Equation (3) would be:

$$x = \frac{-b - \sqrt[3]{M_1} - \sqrt[3]{M_2}}{3a_1}, M_1 = Ab + \frac{3a_1\left(-B + \sqrt{B_2 - 4AC}\right)}{2}, M_2 = Ab + \frac{3a_1\left(-B - \sqrt{B_2 - 4AC}\right)}{2} \tag{4}$$

Thus, from Equation (4), the value of x allows the determination of the PV current as follows:

$$I_{pv} = a\frac{-b - \sqrt[3]{M_1} - \sqrt[3]{M_2}}{3a_1 R_s} \tag{5}$$

To this end, the relations (4) and (5) represent the explicit mathematical equation of the PV SDM. As revealed by the different expressions, the explicit model requires five parameters, namely I_{ph}, I_s, n, R_s, and R_{sh}. To simplify the integration of the explicit PV model (EPVM) into the PVE, these parameters are directly obtained from the actual SDM of the solar panel. Thus, within the PVE, the straightforward computation of Equation (5) serves as a reference current for the system, written as:

$$I_{ref} = f\left(G, T, V_{pve}\right) = a\frac{-b - \sqrt[3]{M_1} - \sqrt[3]{M_2}}{3a_1 R_s} \tag{6}$$

where V_{pve} is the PVE output voltage and G is the solar irradiance in W/m^2. Given that the PVE must operate over a broad spectrum of irradiance, the following relations can be used to compute the photocurrent, saturation current, and shunt resistance for any specific value of G and T [14].

$$I_{ph}(G, T) = \frac{G}{1000}\left(I_{ph-ref} + K_i\left(T - T_{ref}\right)\right) \tag{7}$$

$$I_s(T) = I_{s-ref}\left(\frac{T}{T_{ref}}\right)^3 exp\left[\frac{q}{k}\left(\frac{E_{g,ref}}{T_{ref}} - \frac{E_g}{T}\right)\right], E_g = E_{g,ref}\left(1 - 0.000267\left(T - T_{ref}\right)\right) \tag{8}$$

$$R_{sh}(G) = R_{sh,ref}\left(\frac{1000}{G}\right) \tag{9}$$

where $I_{ph}(G, T)$, $I_s(T)$, and $R_{sh}(G)$ models the environmental dependence of these parameters. Also, E_g is the bandgap energy that varies according to the cell material. AT STC, the reference band gap energy $E_{g,ref}$ for silicon semiconductor material is 1.12 eV [13].

4. Buck Converter and PI Controller Design

To accurately capture the nonlinear dynamics of the PVE, a nonlinear power (DC-DC) converter is employed in the power stage. The proposed PVE uses a buck converter. Among various converter topologies, the buck is chosen for its simplicity, flexibility, lower count of components, and satisfactory efficiency. The electrical structure of the buck converter integrating parasitic components is illustrated in Figure 3. The structure is made up of a power supply DC voltage (input) E, a switch sw, a diode D_2, inductance, and capacitance L_{pve}, C_{pve}. As a practical application, the parasitic components are introduced within these components as r_L and r_c respectively. Provided the converter is well designed, a controller can be employed to force the converter to operate at the desired EPVM reference.

In this paper, we consider a simple proportional integral controller (PI). This controller is chosen for its high simplicity and ease of implementation. Moreover, if properly designed, it can provide a satisfactory response within specific operating conditions.

The structure of the proposed PVE is illustrated in Figure 4. As clearly seen, the PVE features four main inputs. Two of these inputs, i.e., T and G, are manually provided into the system as they represent the desired environmental test conditions. The other two inputs are feedback measurements from the PVE output load R_{pve}, that is V_{pve} and I_{pve}. Thus, the EPVM computes the reference PV current based on the desired G, T, and the feedback measurement V_{pve}. This reference is compared against the actual PVE current.

The resulting error is fed into a PI controller with parameters K_p and K_i. The controller generates the required duty cycle D that is provided as an input to a PWM generator. To regulate the PVE, the PWM control signal is injected at the gate of the converter's switch.
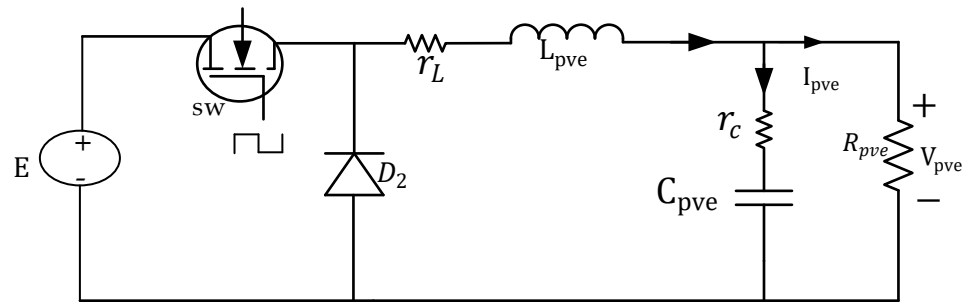

Figure 3. Electrical structure of the practical buck converter integrating parasitic components.
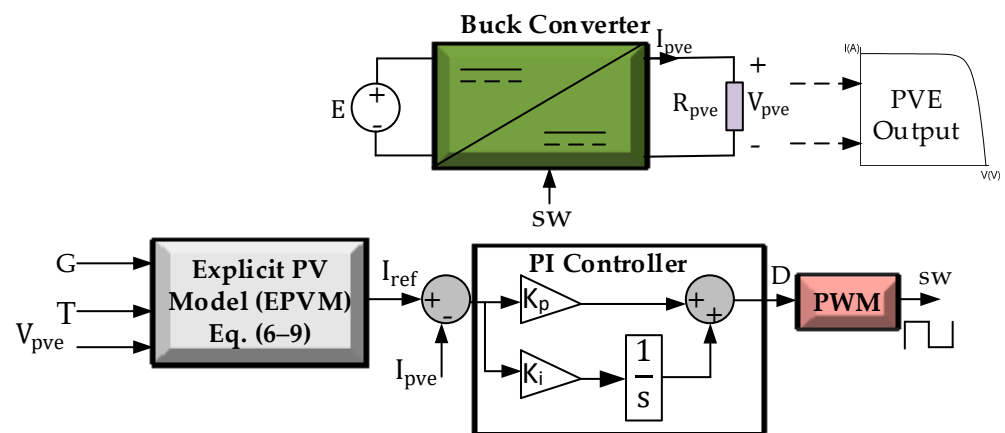

Figure 4. Implementation structure of the proposed PVE.

5. Results and Discussion

A number of experiments are performed to assess the steady state as well as the dynamic performance of the PVE. The PVE is tested on a 200 W solar panel of type KC200GT (Multicrystalline). The manufacturer datasheet of the panel can be found in [14]. The extracted five optimal parameters of the SDM for this panel are $I_{ph} = 8.2288A$, $I_s = 2.3246 \times 10^{-10}$, $n = 0.97736$. $R_s = 0.34483$, $R_{sh} = 150.6921$. A plot of the SDM curves and an experimental measurement obtained from the panel at different experimental conditions as seen in Figure 5 reveals a strong correspondence, endorsing the good accuracy of the SDM.

Also, the buck converter and the PI controller are designed according to [15]. The optimal values of the PI gains are obtained to be $K_p = 0.1163$, $K_i = 32.15$. The parameters of the converter used in this PVE are $L_{pve} = 3.52$ mH, $r_L = 0.631$ Ω, $C_{pve} = 80$ μF, $r_C = 0.134$ Ω. The PWM converter is operated at 31 kHz switching frequency. In order to prevent switching stresses on the power switches at extreme duty cycle, the converter duty cycle is constrained between the lower value $D_{min} = 0.05$ and maximum value $D_{max} = 0.8$.

In order to evaluate the steady-state accuracy of the PVE, the output PVE resistance R_{pve} is varied across the I-V curve in steps of 1.5 Ω. The acquired results are illustrated in Figure 6 revealing a strong agreement between the PVE and the PV model. However, it is seen that the PVE does not span through the entire PV curve. This is because of the duty cycle limitation incorporated into the PVE in order to protect the switches from extreme duty cycle. Although such a constraint is indispensable, it limits the emulation range of the PVE. Thus, in order to stay within an accurate PVE, the output should fall within the emulation range of the PVE. In addition to the steady-state evaluation, the PVE is supposed

to have a swift dynamic response. To assess this feature, the PVE was coupled to different loads at specific environmental conditions.
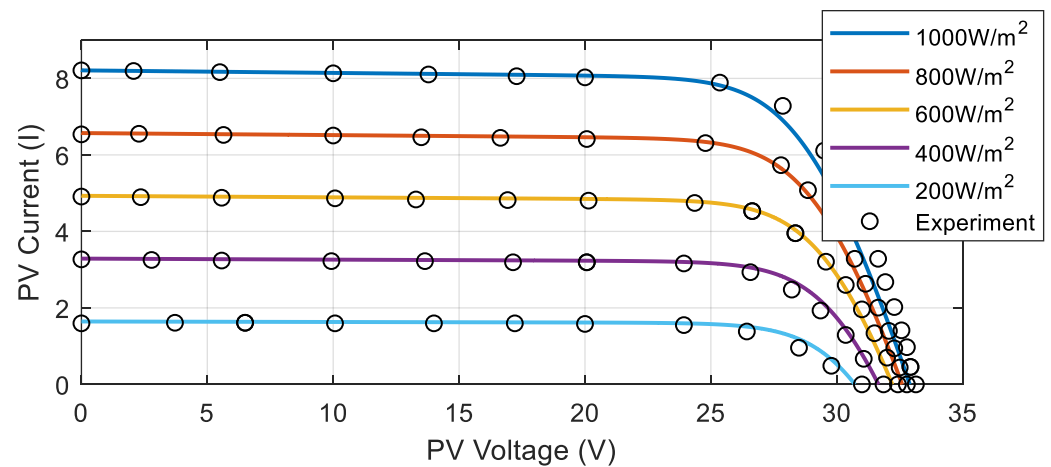

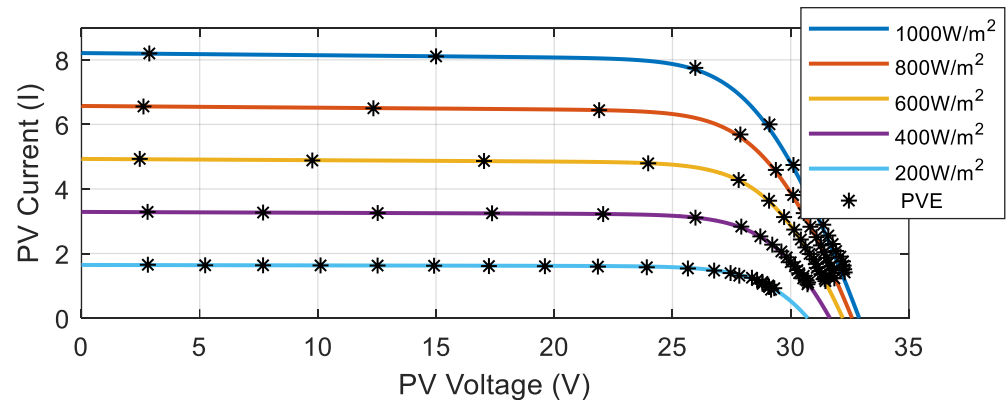**Figure 5.** Plot of the SDM model curves superimposed on experimental data of the actual panel.

Figure 6. Steady state accuracy of the PVE: plot of model curve and emulated points.

Results for the dynamic response assessment of the PVE are illustrated in Figures 7 and 8. It can be seen that the PVE swiftly follows the PV panel with a settling time of less than 20 min in different operating scenarios. Furthermore, the PVE maintains a noticeable dynamic response both in the constant current region (CCR) and constant voltage region (CVR) of the system. However, it is seen that at standard test conditions (G = 1000 W/m^2, T = 25 °C) for conditions corresponding to the CVR the reference current computed by the EPVM has some noticeable oscillations. These oscillations are caused by the oversensitivity of the current PI controller in CVR. This is because for the CVR, a small change in voltage causes a large change in the current. In fact, the sensing variable (voltage) feed to the EPVM is not always stable and has some ripples. In spite of such a challenging scenario, the PVE through the controller still maintains a stable output which aligns consistently with the PV panel as seen in Figure 7 (right) and Figure 8 (right). Thus, such a results reveal a very good dynamic response of the PVE.

The PVE is commonly used for several applications such as the testing of maximum power point tracking [3,16–18]. In such applications, the PVE is supposed to reproduce the dynamic features of the solar panel under varying irradiance levels. Thus, to assess the proposed PVE, the European Standard, MPPT EN 50530 irradiance test profile as presented in Figure 9 is employed. The EN standard recommends irradiance patterns of different gradients. In this test, the irradiance gradient is set at ±80 W/m^2/s for the increasing and decreasing pattern. In order to make the test scenario more rigorous, the irradiance environment is coupled with a varying temperature profile of gradient ±8 °C/s. It can be

seen in Figure 10 that under this test scenario the PVE swiftly follows the solar panel. Thus, this further confirms the suitability of the proposed PVE.
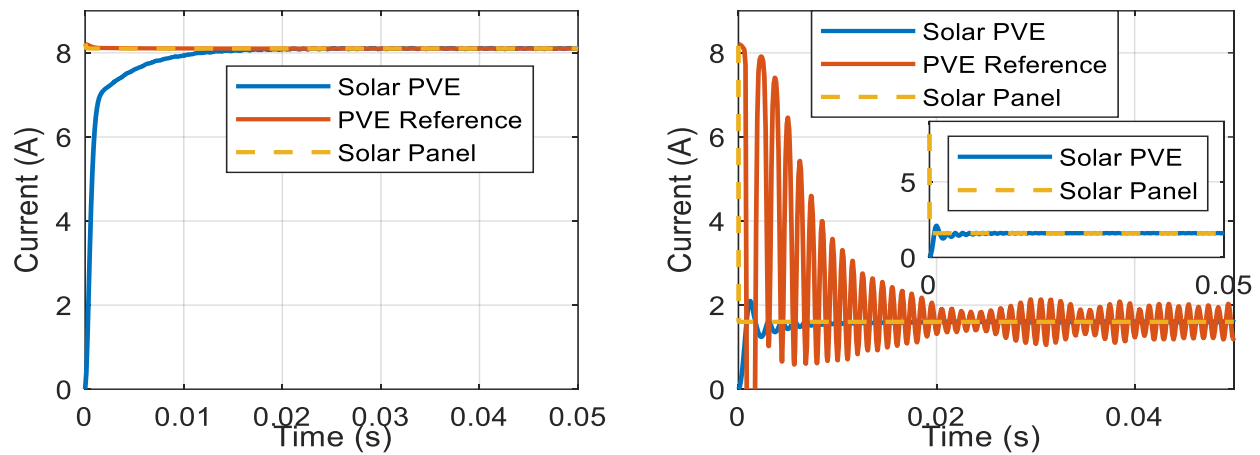

Figure 7. Standard dynamic response of the PVE and actual solar panel at different R_{pve} loads: On the left (CCR operation), $R_{pve} = 2\,\Omega$, on the right (CVR operation) $R_{pve} = 20\,\Omega$.
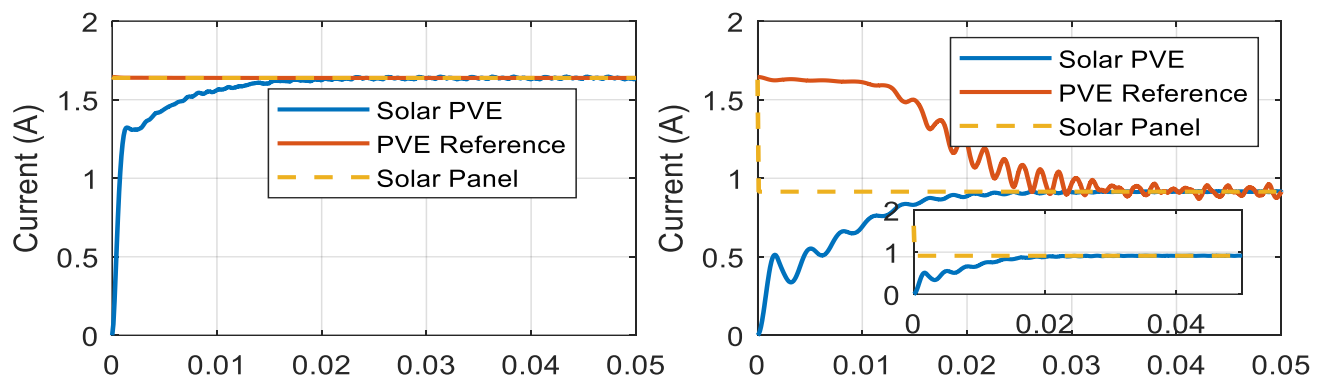

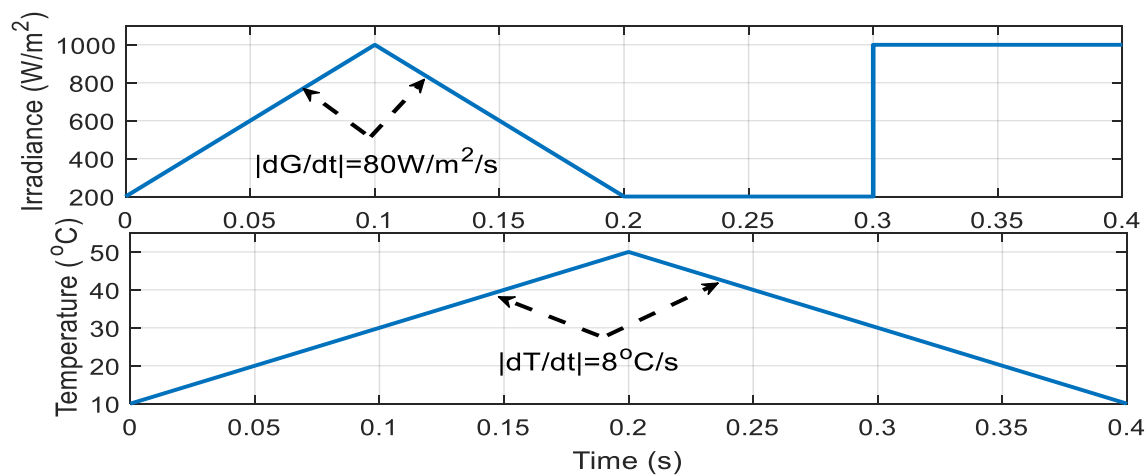**Figure 8.** Dynamic response of the PVE and actual solar panel for $G = 200\,\mathrm{W/m^2}$, at different R_{pve} loads: On the left (CCR operation), $R_{pve} = 3\,\Omega$, on the right (CVR operation) $R_{pve} = 32\,\Omega$.

Figure 9. Environmental test profile: EN 50530 irradiance and varying temperature.
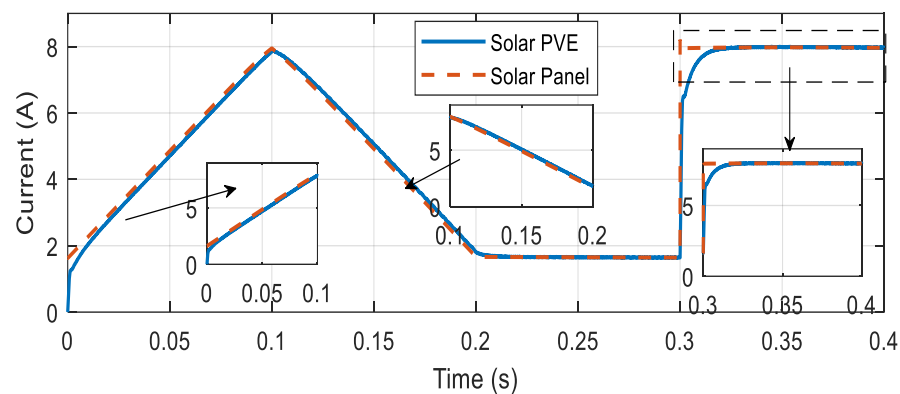
Figure 10. Reponses of the PV panel and the PVE to varying G (EN 50530) and T.

6. Conclusions

This paper has presented a novel approach for the efficient testing of PV systems, emphasizing the importance of thorough controlled testing for their optimal deployment. The proposed PVE technique introduces a simple and straightforward explicit model of the solar panel. Unlike existing methods that rely on iterative computations of complex equations, the proposed PVE eliminates the need for iteration by utilizing explicit computations. This explicit PV model offers remarkable simplicity which in turn contributes to the overall simplicity of the proposed PVE.

The integration of the explicit PV model has consistently demonstrated its simplicity and high flexibility. Through a series of experiments conducted with a 200 W solar panel, the overall PVE presented in this paper has been validated. The obtained results consistently confirm that the proposed PVE effectively emulates the behavior of the solar panel. As a result, this PVE provides a simple and efficient approach for testing PV plants, paving the way for streamlined and effective deployment of PV systems.

Future work based on the above research includes expanding experimental validation of the PVE technique with different solar panel types, capacities, and interconnected systems, while also exploring real-time data integration and comparing the proposed PVE with other testing techniques to assess its advantages and potential improvements.

References

1. Owusu, P.A.; Asumadu-Sarkodie, S. A Review of Renewable Energy Sources, Sustainability Issues and Climate Change Mitigation. *Cogent Eng.* **2016**, *3*, 1167990. [CrossRef]
2. Harrison, A.; Nfah, E.M.; de Dieu Nguimfack Ndongmo, J.; Alombah, N.H. An Enhanced P & O MPPT Algorithm for PV Systems with Fast Dynamic and Steady-State Response under Real Irradiance and Temperature Conditions. *Int. J. Photoenergy* **2022**, *2022*, 6009632. [CrossRef]
3. Harrison, A.; Alombah, N.H. A New High-Performance Photovoltaic Emulator Suitable for Simulating and Validating Maximum Power Point Tracking Controllers. *Int. J. Photoenergy* **2023**, *2023*, 4225831. [CrossRef]

4.   Harrison, A.; Alombah, N.H.; de Dieu Nguimfack Ndongmo, J. A New Hybrid MPPT Based on Incremental Conductance-Integral Backstepping Controller Applied to a PV System under Fast-Changing Operating Conditions. *Int. J. Photoenergy* **2023**, *2023*, 9931481. [CrossRef]

5.   Harrison, A.; de Dieu Nguimfack Ndongmo, J.; Alombah, N.H. Robust Nonlinear Control and Maximum Power Point Tracking in PV Solar Energy System under Real Environmental Conditions. In Proceedings of the ASEC 2022, the 3rd International Electronic Conference on Applied Sciences, Online, 1–15 December 2022; MDPI: Basel, Switzerland, 2022; p. 49.

6.   Alik, R.; Jusoh, A. Modified Perturb and Observe (P & O) with Checking Algorithm under Various Solar Irradiation. *Sol. Energy* **2017**, *148*, 128–139. [CrossRef]

7.   Harrison, A.; Alombah, N.H.; de Dieu Nguimfack Ndongmo, J. Solar Irradiance Estimation and Optimum Power Region Localization in PV Energy Systems under Partial Shaded Condition. *Heliyon* **2023**, *9*, e18434. [CrossRef] [PubMed]

8.   Sudhakar Babu, T.; Mohammed Azharuddin, S.; Nishant, B.; Rajasekar, N. A Dynamic Photo Voltaic Emulator Using DSPACE Controller with High Accuracy Solar Photo Voltaic Characteristics. *J. Renew. Sustain. Energy* **2016**, *8*, 015503. [CrossRef]

9.   Xenophontos, A.; Rarey, J.; Trombetta, A.; Bazzi, A.M. A Flexible Low-Cost Photovoltaic Solar Panel Emulation Platform. In Proceedings of the 2014 Power and Energy Conference at Illinois (PECI), Champaign, IL, USA, 28 February–1 March 2014; pp. 1–6.

10.   Ayop, R.; Tan, C.W. Improved Control Strategy for Photovoltaic Emulator Using Resistance Comparison Method and Binary Search Method. *Sol. Energy* **2017**, *153*, 83–95. [CrossRef]

11.   Ayop, R.; Tan, C.W. A Novel Photovoltaic Emulator Based on Current-Resistor Model Using Binary Search Computation. *Sol. Energy* **2018**, *160*, 186–199. [CrossRef]

12.   Ayop, R.; Wei Tan, C.; Lawan Bukar, A. Simple and Fast Computation Photovoltaic Emulator Using Shift Controller. *IET Renew. Power Gener.* **2020**, *14*, 2017–2026. [CrossRef]

13.   Lun, S.; Du, C.; Guo, T.; Wang, S.; Sang, J.; Li, J. A New Explicit I–V Model of a Solar Cell Based on Taylor's Series Expansion. *Sol. Energy* **2013**, *94*, 221–232. [CrossRef]

14.   Qais, M.H.; Hasanien, H.M.; Alghuwainem, S. Identification of Electrical Parameters for Three-Diode Photovoltaic Model Using Analytical and Sunflower Optimization Algorithm. *Appl. Energy* **2019**, *250*, 109–117. [CrossRef]

15.   Tan, C.W. Buck Converter Design for Photovoltaic Emulator Application. In Proceedings of the 2020 IEEE International Conference on Power and Energy (PECon), Penang, Malaysia, 7–8 December 2020; pp. 293–298.

16.   Hasnaoui, M.; Slama-Belkhodja, I.; Abdelghani, A.B.-B.; Sethom, H.B.A. A Novel and Simple PV Generator Test Procedure for EN50530 Standard Static MPPT Efficiency. In Proceedings of the 2019 Fourteenth International Conference on Ecological Vehicles and Renewable Energies (EVER), Monte-Carlo, Monaco, 8–10 May 2019; IEEE: Toulouse, France, 2019; pp. 1–6.

17.   Nguimfack-Ndongmo, J.d.D.; Harrison, A.; Alombah, N.H.; Kuate-Fochie, R.; Ajesam Asoh, D.; Kenné, G. Adaptive Terminal Synergetic-Backstepping Technique Based Machine Learning Regression Algorithm for MPPT Control of PV Systems under Real Climatic Conditions. *ISA Trans.* 2023, *in press*. [CrossRef] [PubMed]

18.   Harrison, A.; Dieu Nguimfack-Ndongmo, J.d.; Alombah, N.H.; Aloyem Kazé, C.V.; Kuate-Fochie, R.; Asoh, D.A.; Nfah, E.M. Robust Nonlinear MPPT Controller for PV Energy Systems Using PSO-Based Integral Backstepping and Artificial Neural Network Techniques. *Int. J. Dyn. Control* **2023**. [CrossRef]